Measuring Horizontal Ground Deformation Using Optical Satellite Images
Part 2 of 2

Sébastien Leprince

California Institute of Technology

Ge 167 Lecture Notes
May 14, 2009

Measuring Horizontal Ground Displacement, Methodology Review

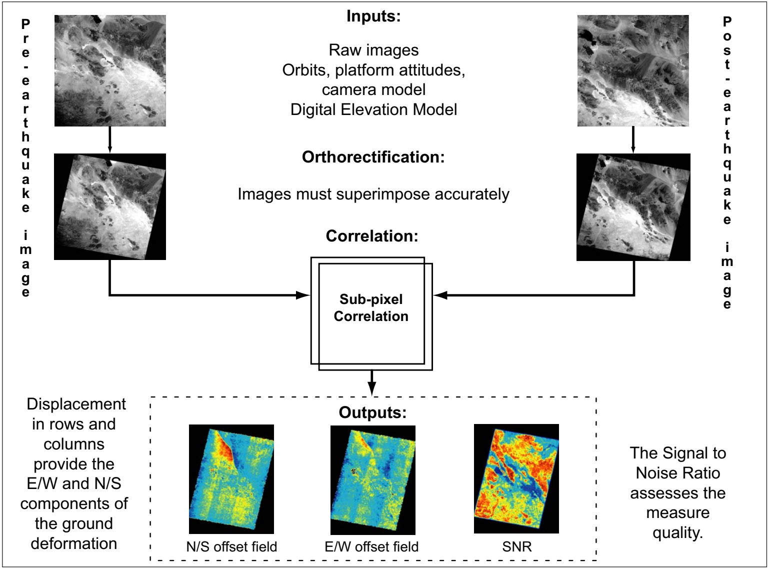

The 1999 Mw 7.1 Hector Mine Earthquake

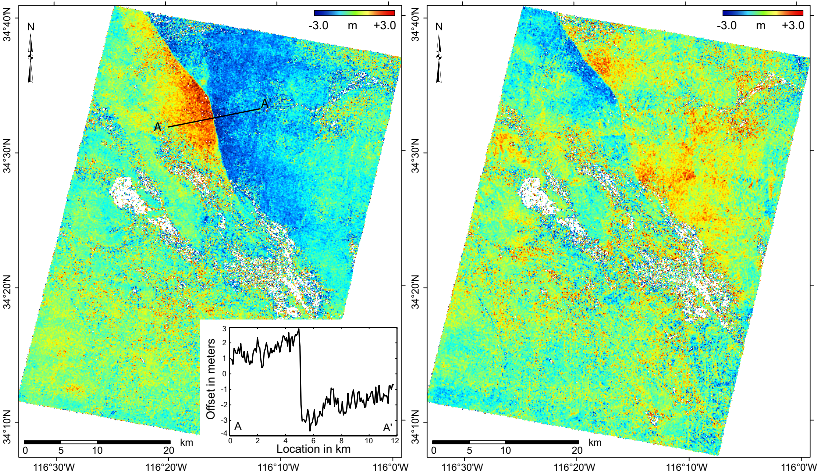

The Hector Mine horizontal coseismic field (NS and EW) derived from 10m SPOT4 1998 and 10m SPOT2 2000 images.

The 1999 Mw 7.1 Hector Mine Earthquake

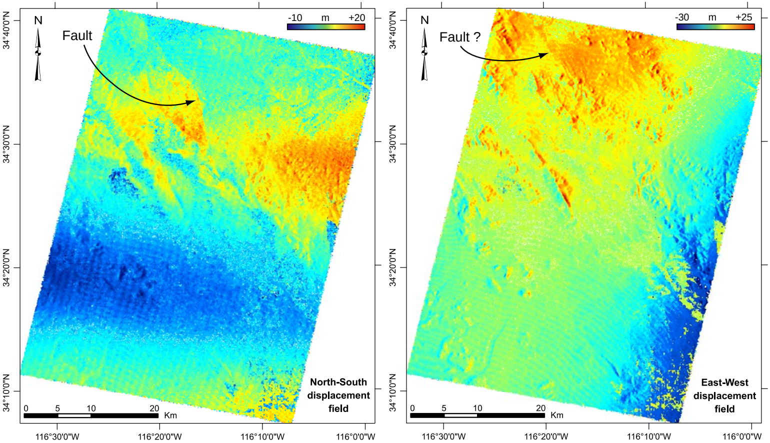

What if instead we measure the above? Do we see the fault discontinuity? Pushbroom satellite: image lines depend on platform variations Topography artifacts due to stereoscopic parallax Parallax due to mis-registration and improper geometrical modeling

Things we should care about for successful correlation:

- Viewing geometry of each pixel has to be physically modeled to account for topography and attitude variations
- Topography and images should be well registered
- Sub-pixel measurement accuracy required $\sim 1/20$ pixel size
- Images co-registration accuracy should be even smaller $\sim 1/50$ pixel size

Geometric Errors: unmodeled platform attitude variations

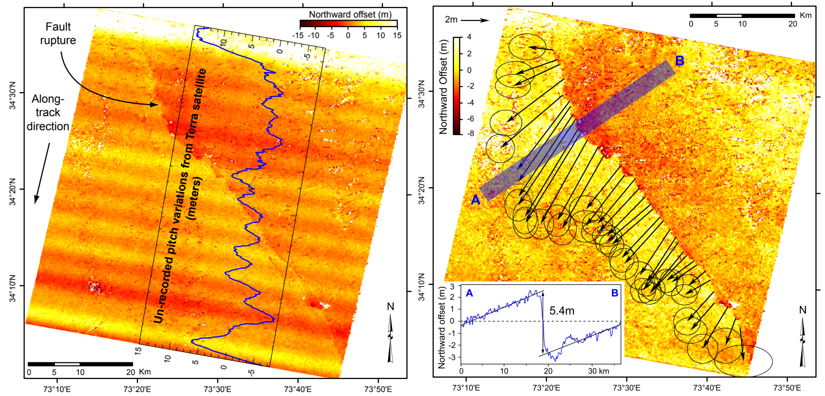

Waves in N-S component of correlation from two ASTER images. Due to unmodeled pitch variations of the Terra satellite. Commonly encountered when processing ASTER images. No good knowledge of platform attitude so difficult to model a priori. Thus far, removal by subtraction from correlation in post-processing.

The 1999 Mw 7.1 Hector Mine Earthquake

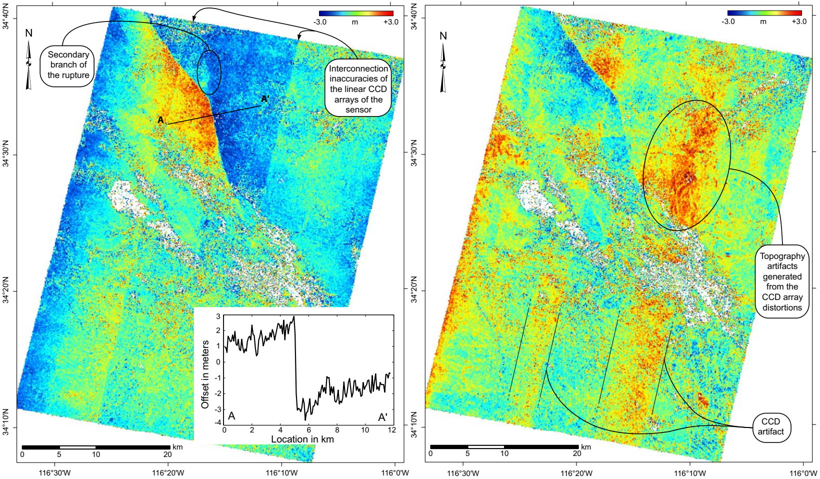

The Hector Mine horizontal coseismic field (NS and EW) showing linear artifacts due to CCD misalignment. The geometry of the CCD sensor has to be well modeled.

The 1999 Mw 7.1 Hector Mine Earthquake

SPOT CCD distortions

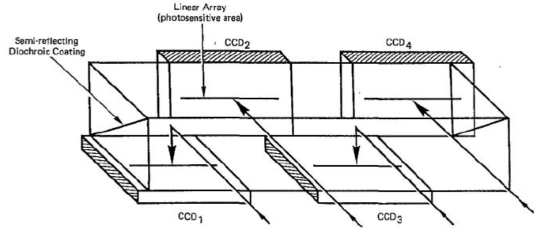

FIGURE 3-9 SCHEMATIC OF A DIVOLI SHOWING FOUR CCD LINEAR ARRAYS

- Optical divider joining the four CCD arrays of the SPOT panchromatic sensor

The 1999 Mw 7.1 Hector Mine Earthquake

SPOT CCD distortions

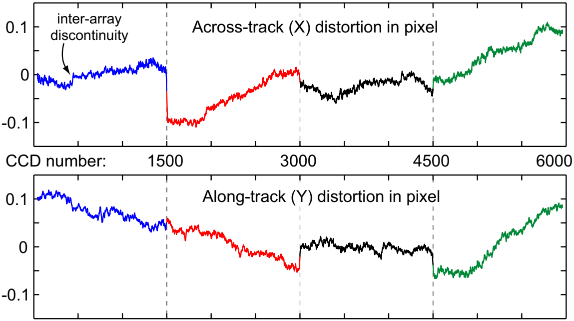

- CCD Calibration model (1/100 pixel accurate) for SPOT 4-HRV1

The 1999 Mw 7.1 Hector Mine Earthquake

SPOT CCD distortions

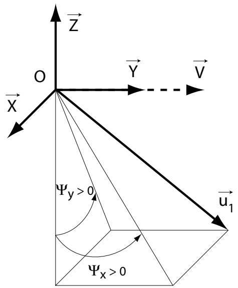

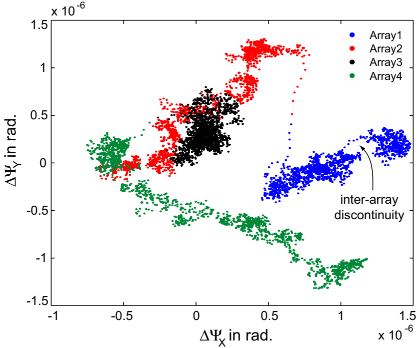

CCD misalignment can be modeled as pointing error on the camera model.

2003 Bam Earthquake using Quickbird and SPOT images

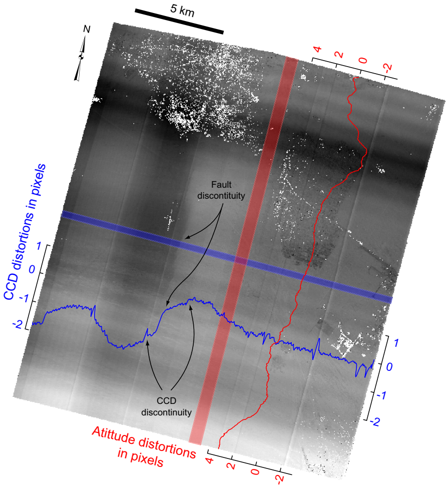

CCD and attitude variations from the Quickbird image

Correlation of HiRISE images from Mars

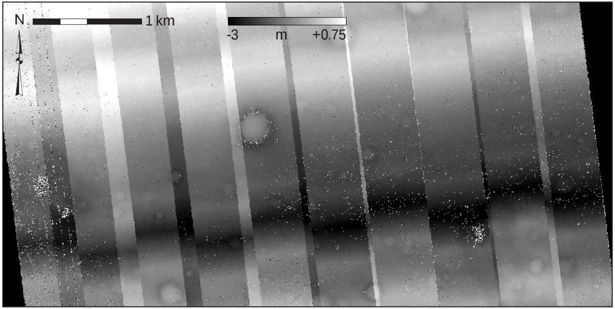

NS displacement of correlation. Result of attitude mis-modeling when CCD lines are misaligned. Correlation artifacts show a phase shift.

Focal plane geometry of modern multispectral sensors

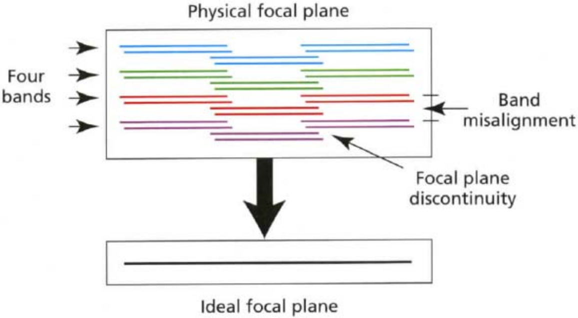

Figure A.22 For the production of multispectral imagery using linear CCD arrays, numerous arrays need to be accommodated in the focal plane of the pushbroom scanner imager. The resulting offsets and shifts need to be corrected later to produce image products with the different spectral band images in correct registration.

This geometry explains the artifacts observed in HiRISE images.

Using archived film images

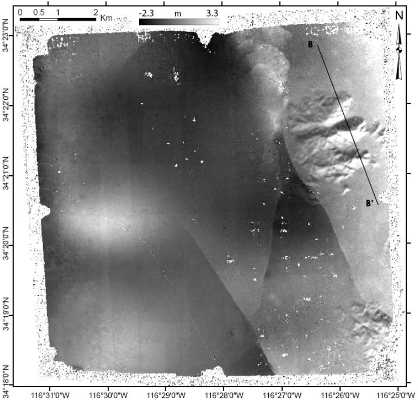

Fig. 3. East/West displacement map of the Landers 1989/1995 correlation. Images were orthorectified on a 1 m grid and correlated using a 64×64 pixel window with a 16 pixel step. Positive displacement is toward the East. Topography and film artifacts are visible on the right and left side of the map respectively. Topographic artifacts are due to a parallax effect caused by the use of a unique DEM for the 1989 and 1995 images although the earthquake changed the topography. Profile BB' is reported on Fig. 10.

Old archived images acquired on film (aerial or declassified spy satellites photographs), have to be scanned to be processed. Film distortions maybe present depending on the film used, film stress during shot, development method, archival conditions, etc... Scanning distortions might also be introduced in the process.

Using archived film images

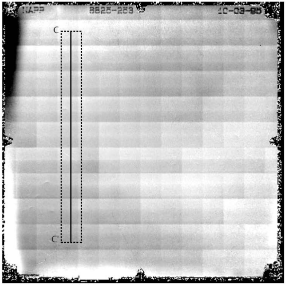

Fig. 11. Displacement map along the line direction of the MD/USGS scans correlation. Scans of the 1995 film were obtained at 21 μm from the USGS and at 10 μm from a MD. MD scan was co-registered and wrapped onto the USGS scan using a sinc kernel for resampling. Correlation used a 64×64 pixel window with a 32 pixel step. Scan artifacts are also visible in the column direction but with smaller amplitude. Profile CC' is reported on Fig. 12. Other long wavelength deformation are due to film distortions and mis-registration.

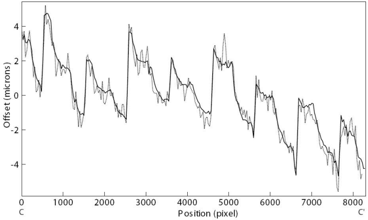

Fig. 12. Profile CC' (Fig. 11) showing scan artifacts with amplitude up to 5 μm (around 20 cm on ground), above the scanner specifications announced at 1.5 μm rmse.

Distortions introduced by the scanner

Geometric error summary

- Unknown or unmodeled attitude variations
- Distortion or misalignment of CCD arrays
- The combination of the two
- If using old frame camera films:
  - Film distortions
  - Scanning distortions
  - Combination of the above two

Topography error: modeling

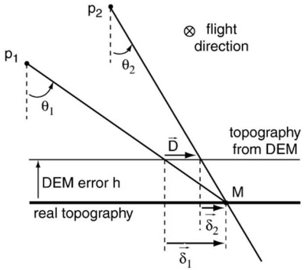

Fig. 2. Effect of DEM-error on displacement measurements. Assume a pixel p_1 from an image I_1 acquired at a date t_1 sees the ground point M, and a pixel p_2 from an image I_2 acquired at a date t_2 sees the same point M on the ground, and that both images are orthorectified and co-registered according to a DEM with an elevation error h. For simplicity, it is assumed that locally, around the ground point M, the topography and the elevation error are well approximated by constants. θ_1 and θ_2 are the angles between the line of sight of pixels p_1 and p_2, and the vertical. When the orthorectified images I_1 and I_2 are correlated, a disparity $D=\delta_1-\delta_2$, induced by the elevation error h, is measured.

$$D = h(\tan(\theta_1) - \tan(\theta_2))$$

- The measurement error $\vec{D}$ results from a trade-off between a well resolved topography and how close the incidence angles of the imaging systems are.
- $\vec{D}$ lives in the plane $(p_1 M p_2)$, called the epipolar plane. For pushbroom systems, this plane is generally in the across-track direction, hence EW components are usually affected the most by topo biases.

Topography error: dramatic examples

50 cm resolution aerial images orthorectified with 40 m DEM, which has been interpolated using nearest neighbor method.

Topography error sources

- DEM with insufficient vertical resolution
- DEM with insufficient horizontal resolution
- Change of topography between acquisitions not accounted for during orthorectification (large earthquakes, glacier thickness, etc...)
- Mis-registration between image and DEM. During orthorectification, pixels are not projected on the ground where they should be (because of errors or approximations in viewing geometry modeling?)
- Multiple combinations of above reasons

Influence of Ground Control Points

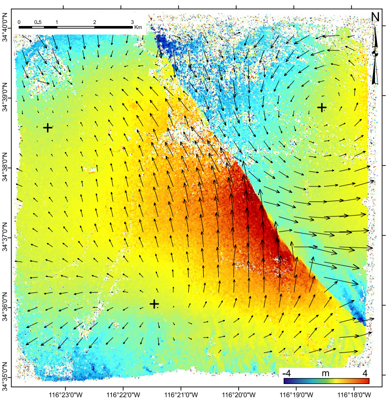

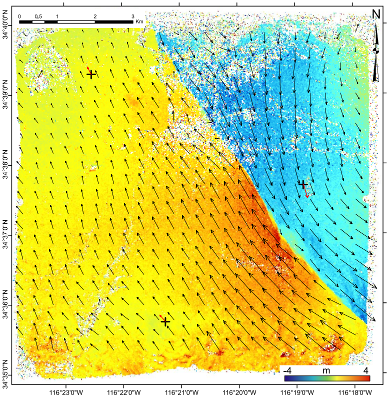

- Aerial photographs (1 m)
  USGS-NAPP
  7/25/89 - 06/01/02

- Introducing SPOT offsets allows to solve for longer deformation wavelength

When does correlation fail?

- When, at the scale of the correlation window, landscape has dramatically changed

When does correlation fail?

- When, at the scale of the correlation window, shadows orientation have dramatically moved. Imaging satellites are sun-synchronous, only sensitive to seasonal variations. Aerial photographs may present larger shadowing difference, no time constraint.

When does correlation fail?

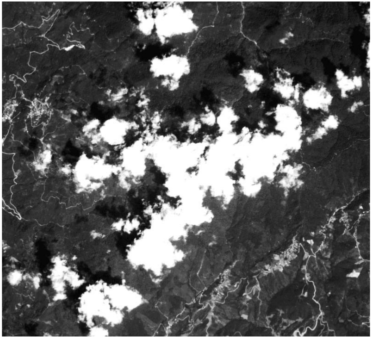

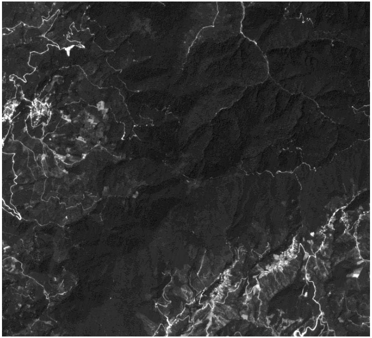

- When, at the scale of the correlation window, cloud coverage, and cloud casted shadows are different.

When does correlation fail?

Correlation fails when, at the scale of the correlation window:

- Landscape has dramatically changed (new buildings or constructions, new alluvions)
- Shadows have dramatically changed (mountainous terrain, tall buildings, poles, etc...)
- Cloud or snow cover changes
- Images acquired in difference spectral bands (objects may or may not be visible in some spectral bands)
- Occlusion of objects (behind buildings, behind clouds, etc...)

Generally, correlation will fail when, at the scale of the correlation window, your eyes cannot recognize the images to be compared.

Correlation noise modeling

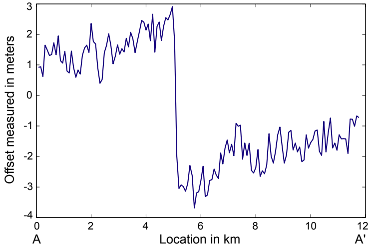

Profile AA′ from NS correlation image. Maximum displacement of 6 m in the NS direction. High frequency noise accounts for about 80-85 cm.

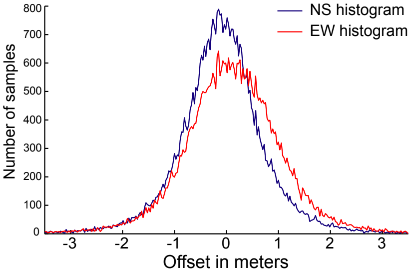

- μ_{NS} = -7.4 cm σ_{NS} = 82 cm
- μ_{EW} = 18.3 cm σ_{EW} = 92 cm

Correlation noise modeling

Correlation noise can be modeled with two additive components:

- When correlation works: Additive white Gaussian noise with standard deviation around 1/10 of the image pixel size. Noise due to slight changes in landscape, radiometric quantization, aliasing from optics.
- When correlation does not work: impulse noise. The displacement takes a value which is uniformly distributed between $-\frac{N}{2}$ and $\frac{N}{2}$ if N is the size of the correlation window.

Correlation noise modeling: why should we care?

- The noise distribution is Gaussian-like (symmetrical and centered at zero), therefore measurements in each EW or NS components can be averaged. The mean is an unbiased estimator. Opens the way to denoising algorithms.

- Because the noise is not correlated with the signal to be measured, the projection of the vector field onto any direction independent of the noise will also keep the same noise characteristics. Then we can project the vectors along profiles and stack them to produce denoised measurements.

- If X and Y are two independent random variables following a normal distribution with variance σ, then the magnitude given by $\sqrt{X^2 + Y^2}$ will follow a Rayleigh distribution with mean $\mu = \sigma\sqrt{\frac{\pi}{2}}$. Therefore, the magnitude of a displacement (e.g., the flow velocity of a glacier, a landslide, or sand dunes migration rates, etc...), cannot be directly studied through the Euclidean norm of the correlation measurements. The magnitude will be overestimated by a value close to μ. These measurements should either be denoised to an acceptable level first, or should be studied along a given projection (projection along a flow line or the most likely flow direction, etc...).

Post-processing: Denoising via Non-Local Means

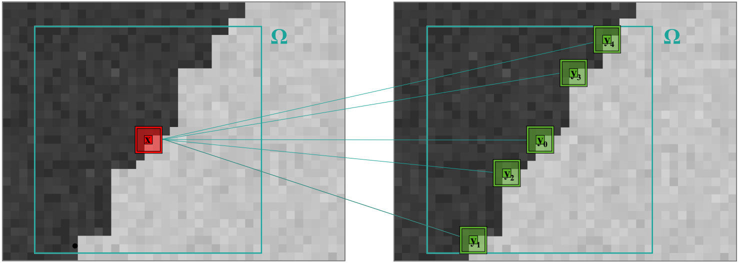

- Average of pixels with similar configuration:

$$NL_h[u](\mathbf{x}) = \frac{1}{C(\mathbf{x})} \int_\Omega e^{-\frac{1}{h^2} \int_{\mathbb{R}^2} G_a(t) |u(\mathbf{x}+t) - u(\mathbf{y}+t)|^2 dt} \; u(\mathbf{y}) \; d\mathbf{y}$$

- G_a Gaussian kernel of standard deviation a
- h filtering parameter

Buades, et al., IJCV, 2008

Post-processing: Denoising via Non-Local Means

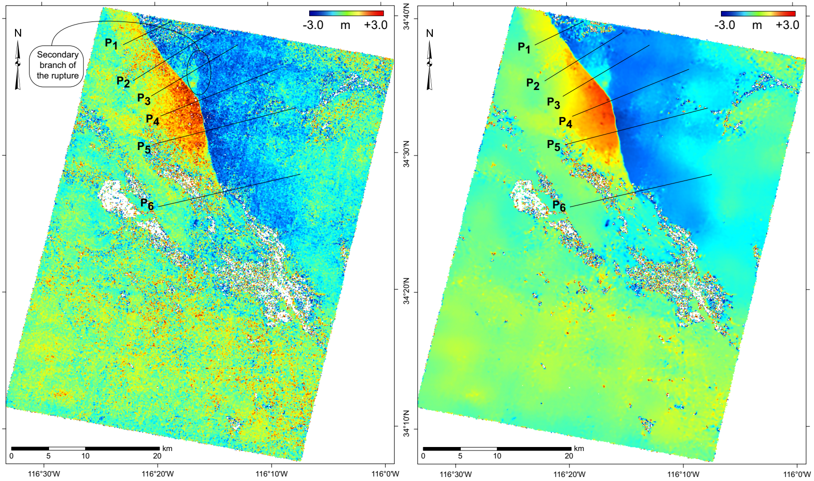

- Correlation from SPOT 10 m images
- Denoising of the NS component of the displacement field induced by the Hector Mine earthquake.

Post-processing: Denoising via Non-Local Means

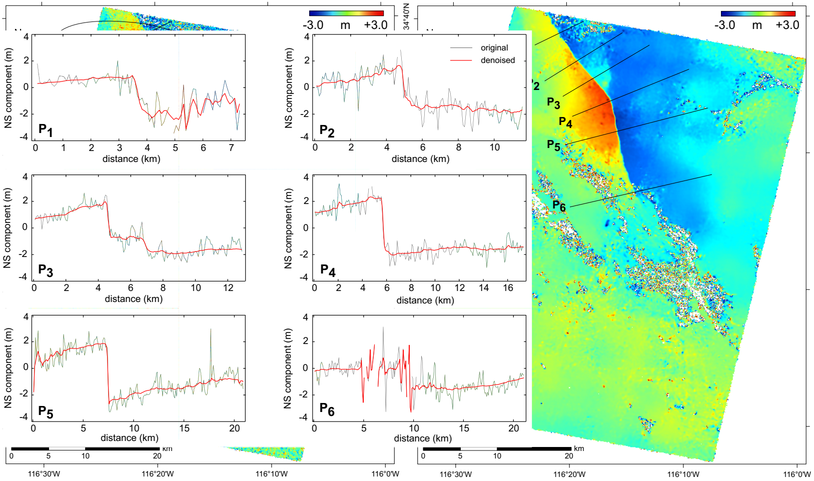

- Correlation from SPOT 10 m images
- Denoising of the NS component of the displacement field induced by the Hector Mine earthquake.

Examples :The 1992 Mw 7.3 Landers Earthquake, CA

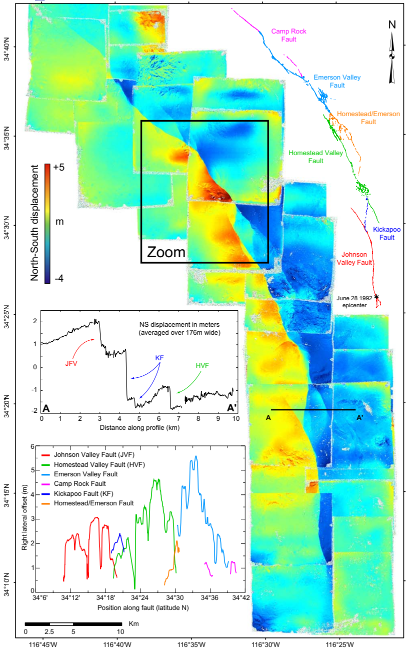

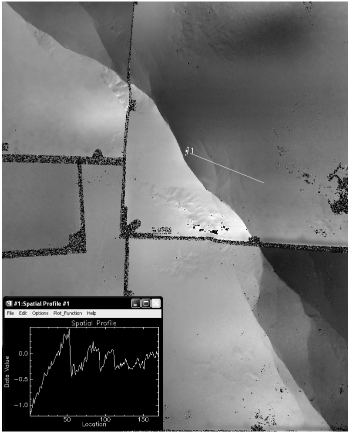

NS component - 30 pairs air photos from USGS - 1989-1995

SPOT5 used as reference

Collaboration F. Ayoub, Caltech, and Y. Klinger, IPG

Paris, France

Example: The Mer de Glace Glacier, France

SPOT 5 images 2.5 m resolution
2003-08-23
2003-09-18

Example: The Mer de Glace Glacier, France

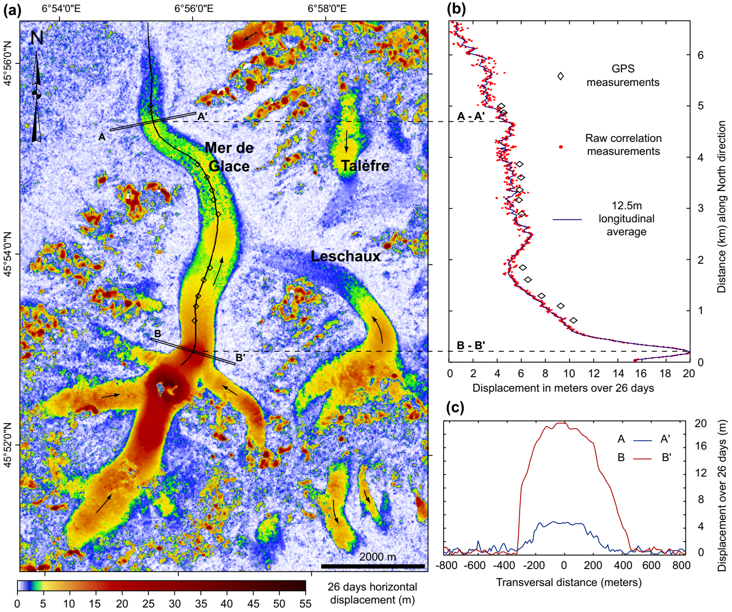

Processing Chain

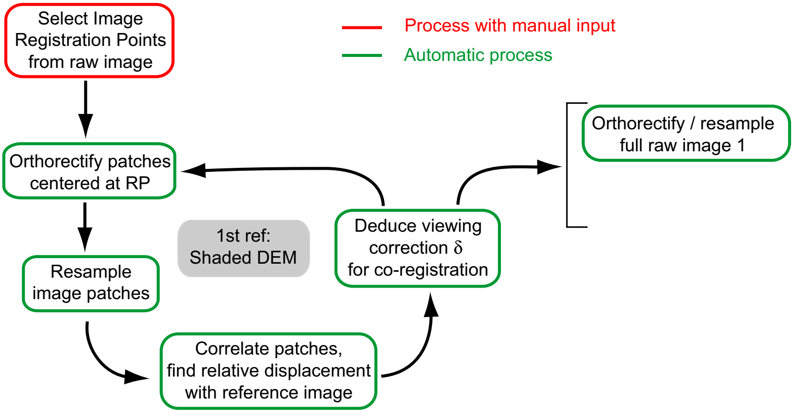

Processing Chain

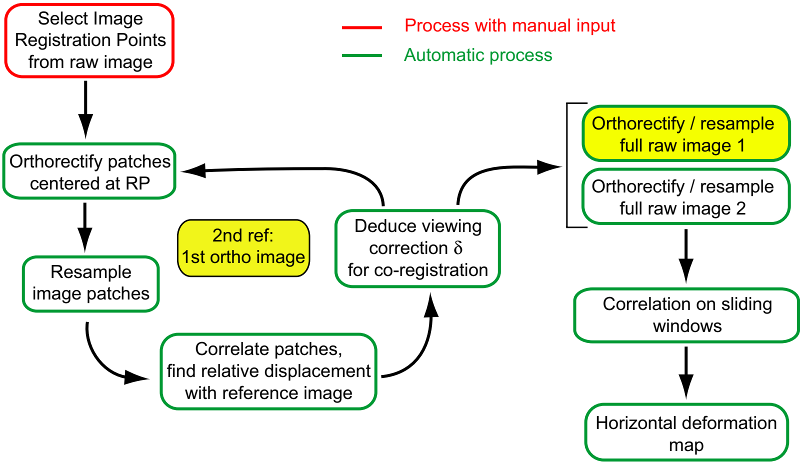

COSI-Corr

- COSI-Corr (Co-registration of Optically Sensed Images and Correlation), ENVI toolbox available for download since 2007 from Caltech TO website.
  - Aerial photos
  - All SPOT (1,2,3,4,5) satellites (all spectral bands)
  - ASTER instrument (all spectral bands)
  - Quickbird satellite images (all spectral bands)
  - Correlation denoising via NL-Means algorithm
- More coming soon, stay tuned!

To use COSI-Corr, you will have to:

- Compute the ancillary file for your sensor (regroups the metadata from your sensor into one single file to be used during processing)
- Select GCPs between the raw slave image (to be processed), and a reference ortho-image (master image)
- Optimize the GCP according to the Master image. This step will also produce an optimized viewing geometry for the slave image so that it will be well registered with the master once it's orthorectified
- Ortho-rectify/resample the raw slave image using the optimized GCP. The slave ortho-image should now be well registered with the master ortho-image
- Repeat the previous steps for several images. The slave ortho-image becomes the new reference for subsequent processing
- Run the correlation between orthorectified and registered images. The correlation window size should not be smaller than 32x32 pixels, and should be larger than twice the largest displacement to be measured. A multiscale approach can be selected. The correlation step determines the spatial resolution of the measurements
- Displacement field is ready to be analyzed. Check for noise level, geometry errors, etc... Usually a good idea to discard measurements with low SNR and large unphysical values.
- More during lab and in the COSI-Corr user's guide.

The End: Thank you!

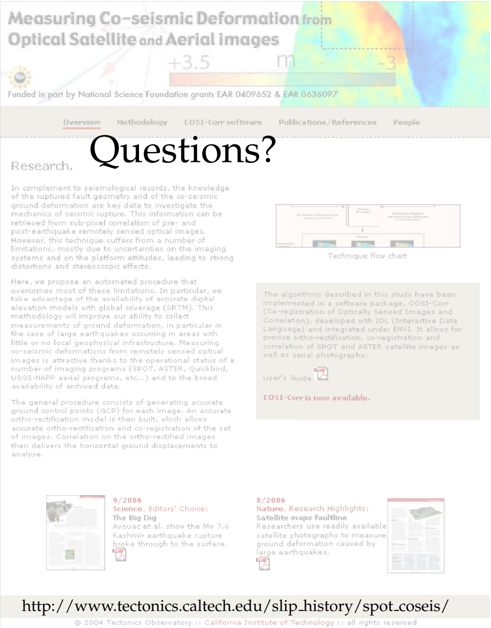

Measuring Co-seismic Deformation from Optical Satellite and Aerial images

Funded in part by National Science Foundation grants EAR 0409652 & EAR 0636097

Overview Methodology COSI-Corr software Publications/References People

Research.

In complement to seismological records, the knowledge of the ruptured fault geometry and of the co-seismic ground deformation are key data to investigate the mechanics of seismic rupture. This information can be retrieved from sub-pixel correlation of pre- and post-earthquake remotely sensed optical images. However, this technique suffers from a number of limitations, mostly due to uncertainties on the imaging systems and on the platform attitudes, leading to strong distortions and stereoscopic effects.

Here, we propose an automated procedure that overcomes most of these limitations. In particular, we take advantage of the availability of accurate digital elevation models with global coverage (SRTM). This methodology will improve our ability to collect measurements of ground deformation, in particular in the case of large earthquakes occurring in areas with little or no local geophysical infrastructure. Measuring co-seismic deformations from remotely sensed optical images is attractive thanks to the operational status of a number of imaging programs (SPOT, ASTER, Quickbird, USGS-NAPP aerial programs, etc...) and to the broad availability of archived data.

The general procedure consists of generating accurate ground control points (GCP) for each image. An accurate ortho-rectification model is then built, which allows accurate ortho-rectification and co-registration of the set of images. Correlation on the ortho-rectified images then delivers the horizontal ground displacements to analyse.

Technique flow chart

The algorithms described in this study have been implemented in a software package, COSI-Corr (Co-registration of Optically Sensed Images and Correlation), developed with IDL (Interactive Data Language) and integrated under ENVI. It allows for precise ortho-rectification, co-registration and correlation of SPOT and ASTER satellite images as well as aerial photographs.

User's Guide

COSI-Corr is now available.

9/2006
Science, Editors' Choice:
The Big Dig
Avouac et al. show the Mw 7.6 Kashmir earthquake rupture broke through to the surface.

8/2006
Nature, Research Highlights:
Satellite maps faultline
Researchers use readily available satellite photographs to measure ground deformation caused by large earthquakes.

Questions?

http://www.tectonics.caltech.edu/slip_history/spot_coseis/

COSI-Corr
web site

The La Valette Landslide, France

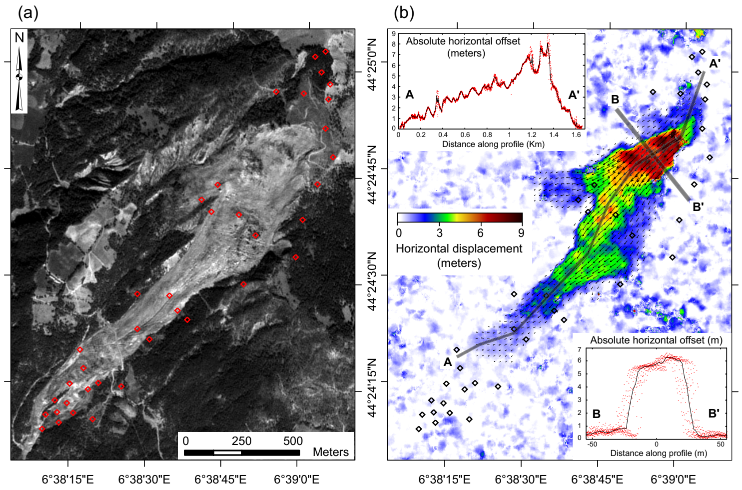

SPOT5 2.5m resolution images, 09/19/2003 - 08/22/2004

S. Leprince, et al., EOS, 2008

The Great Sand Dunes, Colorado

The Great Sand Dunes, Colorado

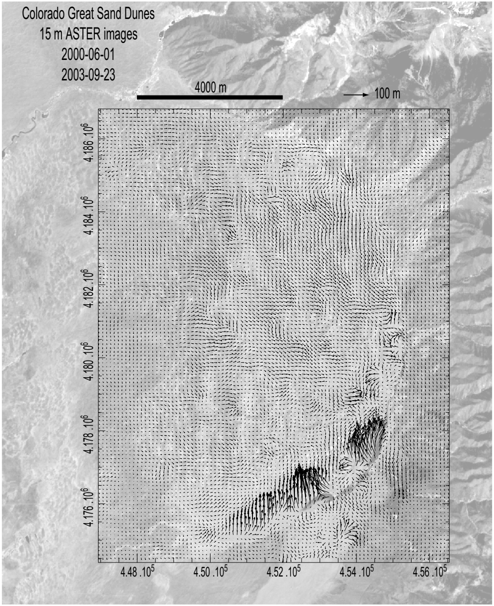

Technique limitation:

Aliasing

- Optical cut-off frequency ≈ 4-5 times the CCD Nyquist frequency on SPOT 1-4
- Can be formalized as a super-resolution pb for the correlation
- Aliasing could be avoided by defocusing of proper adjustment of the bias voltage in back illuminated CCD (would required deconvolution to recover sharp image)

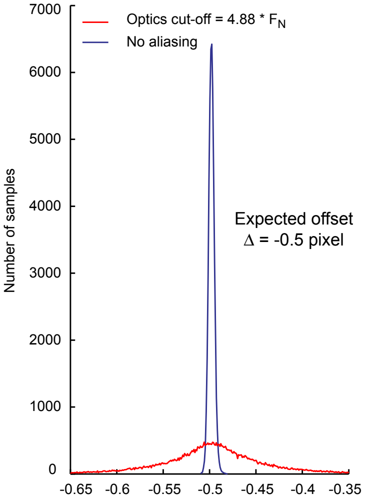

- $\mu_{noalias}$ = - 0.498 $\sigma_{noalias}$ = 0.002
- μ_{alias} = - 0.496 σ_{alias} = 0.07

The AFAR rift in Ethiopia, 2005 events

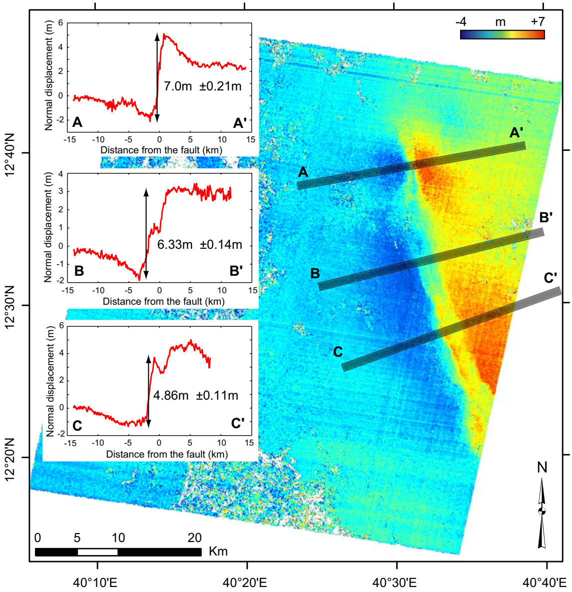

EW displacement field, from 10m SPOT 4 images, 12/19/2004 01/13/2006

Collaboration I. Barisin and B. Parsons, University of Oxford, UK

The 1999 Mw 7.4 Izmit and Mw 7.2 Duzce Earthquakes

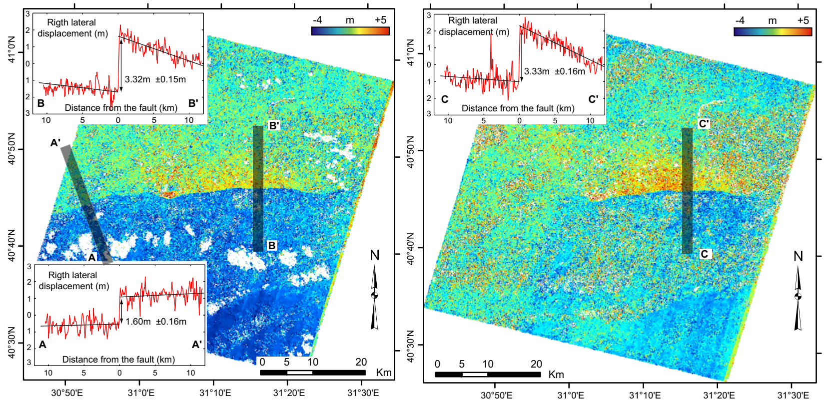

EW component of displacement field, from 10m SPOT images acquired on 21/06/1999, 03/10/1999, and 12/07/2000

Collaboration A.O. Konca and D. Helmberger, Caltech

Sand Dunes Migration, Morocco

Laayoun, Maroc

ASTER images acquired in 2001 and 2006

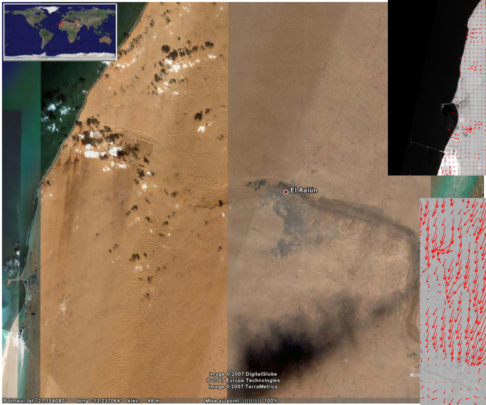

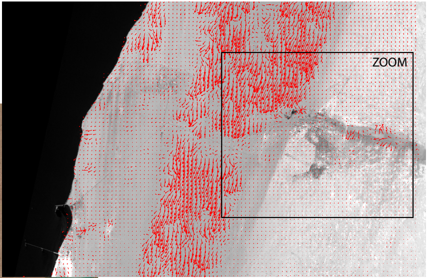

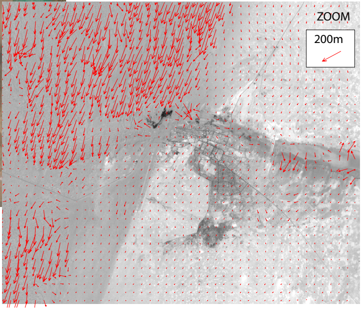

Collaboration, Mohamed Chlieh, IRD, France